Two-Particle Coulomb Green Function Method with Projected Potential: Application to He Double Photoionization†

Luca Argenti* and Renato Colle‡

Dipartimento di Chimica Applicata e Scienza dei Materiali (DICASM), Università di Bologna, via del Lazzaretto 15/5, I-40136 Bologna, Italy

Received: June 2, 2009; Revised Manuscript Received: July 22, 2009

A new method to compute fully differential double photoionization cross sections of atoms has been devised and fully developed for two-electron systems. The method exploits the Green function for two noninteracting electrons in the field of a nuclear charge to infer the effects of the residual potential projected on a set of L^2-basis functions. Test calculations on helium at 100 eV excess energy indicate that, as long as the relevant part of the interaction potential is accounted for, the fully differential cross sections calculated in acceleration and velocity gauges converge in absolute value and reproduce measured angular distributions with a tunable accuracy. Generalization of the method to treat double photoionization of many-electron atoms is sketched.

I. Introduction

Since its first measurement in 1993,[1] the single-photon triple-differential cross-section (TDCS) of helium double photoionization (DPI) has been the subject of extensive theoretical and experimental investigations. Now its phenomenology and fundamental mechanisms have been well established,[2] and TDCS of many-electron atoms are probably the next, more challenging target of the theoretical investigation. In this context, experimentalists have already recorded DPI cross sections of s and p shells in heavier noble gases, and peculiar characteristics have emerged that still await an accurate theoretical explanation. To mention just two of them: the interference between direct double photoionization channels of different symmetries[3] and between direct and indirect channels.[4]

From the theoretical point of view, double photoionization, together with the similar process of electron-impact ionization, is a formidable task because of its sensitivity to correlation, its small cross sections compared to the dominant single ionization channels, and the complexity of the appropriate boundary conditions.[5−7] Most of the methods which proved successful in describing breakup of two-electron systems either cannot be readily applied to many-electron atoms, or require huge numerical resources.

We propose here an essentially novel approach to double photoionization, which yields sufficiently accurate results for helium TDCS with a modest computational effort: a method that contains internal parameters that allow to tune the quality of the calculation to the required degree of accuracy and can be extended also to the study of DPI of many-electron atoms. For comparison with the existing techniques, we shall first survey briefly the most prominent among them, and then describe our method with applications to helium DPI.

Considerable effort has been spent in the early nineties to formulate analytical expressions for the final wave function of three charged particles that incorporate explicitly some aspects of the complicated asymptotic behavior of the full fragmentation channel. Despite some success, particularly with the three Coulomb-wave (3C) approach,[8−10] a close scrutiny[11,12] eventually concluded that even the most sophisticated among these methods usually yield inaccurate results, with few exceptions due to fortuitous agreement with experiment. It was realized that any successful method could not avoid heavy calculations and should somehow circumvent the prohibitive three-body breakup boundary conditions.

Following this direction, Shakeshaft et al. proposed an approach[13,14] in which the final wave function is expressed as a product of two screened Coulomb-wave functions (2SC) plus a localized component to correct for short-range interactions among the three charged particles. Unfortunately, the obtained cross section relies on the summation of a divergent series which presents serious numerical problems (see, e.g., ref 15). The method was therefore abandoned.

Nowadays, there are four main methods[16] well describing the physics of helium single-photon double-ionization processes: the Hyperspherical R-Matrix with Semiclassical Outgoing Waves (H$\mathscr{R}$M-SOW), the Time Dependent Close Coupling (TDCC), the Convergent Close Coupling (CCC), and the Exterior Complex Scaling (ECS) method.

In the H$\mathscr{R}$M-SOW method, proposed by Malegat et al.,[17] the hyperangular variables are discretized and the R-matrix solution within an hypersphere of radius R_0 is semiclassically propagated outward up to a certain hyper-radius, where the outgoing flux is evaluated. This method gives very good results for helium DPI[18−20] but is numerically very demanding. Flux-extrapolation methods are known indeed to be inherently slowly convergent, even for short-range interactions,[21] since the required asymptotic form is approached at distances much larger than the interaction range itself.[22] Furthermore, H$\mathscr{R}$M-SOW requires large distances also to confine the contribution of single ionization channels, and, more seriously, hyperspherical coordinates cannot be readily matched to ordinary spherical coordinates, a fact that hinders the extension of H$\mathscr{R}$M-SOW to many-electron atoms. (See, e.g., ref 23 for beryllium DPI).

The Time Dependent Close Coupling method, introduced initially to deal with (e, 2e) processes,[24] has been extended in the late nineties to (γ, 2e) processes for obtaining total[25] and

† Part of the "Vincenzo Aquilanti Festschrift".

* Electronic address: luca.argenti@gmail.com. Present address: Atomic Physics, Fysikum, Stockholm University, AlbaNova University Center, SE-106 91 Stockholm, Sweden.

‡ Electronic address: colle@sns.it.

10.1021/jp905155w
Published on Web 08/31/2009

fully differential[26,27] helium DPI cross sections. The authors devised a method to extract the differential cross section from the time dependent scattering component of the wave function;[28] this method circumvents the bottleneck of a slowly convergent outgoing flux, but still relies on lattice techniques which require very large computational resources to provide accurate results. The extension of TDCC to many-electron atoms seems not easy to be realized. (See, e.g., ref 29 for beryllium DPI).

The Convergent Close Coupling method,[30] initially introduced by Bray and Stelbovics in the frame of the two-body scattering problem, was recognized as a useful tool also for the three-body problem,[30] yielding accurate total ionization cross sections for both (e, 2e)[31] and (γ, 2e) processes.[32] CCC was later shown to be able to reproduce also multiple-differential cross sections.[33−35] Despite its success, the CCC method attracted some criticism:[36] its use to obtain differential cross sections appears essentially justified on practical evidence and heuristic speculations, rather than sound mathematical arguments, and its convergence is inherently slow due to the effort of approximating a generally discontinuous single differential cross section.[37] Because of this fact, very large computational resources are needed to obtain converged results, as pointed out also by Bray himself.[38]

Finally, the Exterior Complex Scaling method[39] solves the Lippmann−Schwinger equation of the scattering problem in a form where the sought solution is expressed entirely in terms of its asymptotic form for (e, 2e) processes, or in terms of the driven Schrödinger equation for (γ, 2e) processes. The appropriate Green function, regular on the real axis and with the required outgoing-wave boundary conditions, is obtained by inverting the projected ($E - H_\theta$) operator, where H_θ is a "complex rotated" Hamiltonian. When applied to helium DPI, ECS yields TDCS in excellent agreement with the experiment[40,16] but, for many-electron atoms, the "all outgoing" criterion applied to the driven Schrödinger equation may prove inadequate. It is not clear, indeed, how to extract from the full scattering function the amplitudes of the different channels when the grandparent ion may emerge in an excited state. At the moment, this drawback is common to all the proposed complex scaling techniques,[41] that lose track of branching ratios and, consequently, of partial cross sections when applied to many-electron atoms.

The method we present here is a generalization of that proposed in ref 42. It utilizes an unperturbed two-electron reference channel in which the interelectronic repulsion is neglected altogether and the two outgoing electrons are treated on equal footing. The eigenfunctions of this channel are suitably coupled products of one-electron functions in the field of the grandparent ion. The interelectronic interaction is then introduced as a projected potential, well represented by a set of B-spline functions up to a relatively large radius (few tens of atomic units), where the kinetic energy of the outgoing electrons is expected to be large in comparison with their mutual potential energy (for a large part of the angular domain of interest). Using a projected potential, the scattering problem with outgoing-wave boundary conditions in the double ionization channel can be formulated in terms of a solvable Lippmann-Schwinger equation.

The present method is similar to CCC, in that it uses a close-coupling approach but differs from CCC since the two electrons are treated on equal footing. The method is also similar to ECS since it solves a Lippmann−Schwinger equation with suitable choice of the boundary conditions. The difference is that our method utilizes an unperturbed Green function defined exploiting the identity resolution on a complete set of two-electron functions for the bound−bound, bound-continuum and continuum-continuum parts of the spectrum. The matrix elements of the unperturbed Green function are then computed on a basis set of B-splines.

A major advantage of this method is also that its procedures are well-defined not only for two-electron systems (in which case the appropriate Green function is the two-particle Coulomb Green function) but also for many-electron systems, for which the state of the grandparent ion can be suitably represented by a determinantal function orthogonal to the continuum channel.

II. Theoretical Method

The triple differential cross section for the double photoionization of a bound state (ϕ_0) to a final state (α) of the grandparent ion with two outgoing electrons of momentum $\vec{k}_1, \vec{k}_2$ and spin projection σ_1, σ_2, respectively, is given by

$$\frac{\mathrm{d}\sigma}{\mathrm{d}E_1\,\mathrm{d}\Omega_1\,\mathrm{d}\Omega_2} = \frac{4\pi^2}{c\omega} k_1 k_2 |\langle \psi^-_{\alpha,\vec{k}_1\sigma_1\vec{k}_2\sigma_2} | \mathcal{O}_1 | \phi_0 \rangle|^2 \qquad (1)$$

where, in dipole approximation, the transition operator is $\mathcal{O}_1 = \hat{\epsilon} \cdot \sum_{i=1}^{N} \vec{\nabla}_i$, with N being the number of electrons and $\hat{\epsilon}$ the photon polarization vector.

Huetz et al. derived[43] the following TDCS expression for a linearly polarized incident light

$$\frac{\mathrm{d}\sigma}{\mathrm{d}E_1\,\mathrm{d}\Omega_1\,\mathrm{d}\Omega_2} = |a_\mathrm{g}(k_1, k_2, \theta_{12})(\cos\theta_1 + \cos\theta_2) + a_\mathrm{u}(k_1, k_2, \theta_{12})(\cos\theta_1 - \cos\theta_2)|^2 \qquad (2)$$

where a_g and a_u are complex amplitudes, symmetric and antisymmetric upon interchange of the two energies. The dependence of these coefficients on θ_{12} can be expressed exactly in terms of Legendre polynomials and reduced matrix elements:[44,45]

$$a_{\mathrm{g/u}}(k_1, k_2, \theta_{12}) = \sum_l C_l^{\pm}(\theta_{12}) A^{\mathrm{g/u}}_{l+1 k_1 l k_2} \qquad (3)$$

where

$$C_l^{\pm}(\theta_{12}) = (-1)^l \frac{\sqrt{l+1}}{4\pi} \frac{P_l(\cos\theta_{12}) \pm P_{l+1}(\cos\theta_{12})}{(1 \pm \cos\theta_{12})} \qquad (4)$$

and

$$A^{\mathrm{g/u}}_{l_1 k_1 l_2 k_2} = \sqrt{\frac{\pi k_1 k_2}{3c\omega}} (\langle \psi^{-^1\mathrm{P^o}}_{\alpha; l_1 k_1 l_2 k_2} || P_1 || \phi_0 \rangle \pm \langle \psi^{-^1\mathrm{P^o}}_{\alpha; l_1 k_2 l_2 k_1} || P_1 || \phi_0 \rangle) \qquad (5)$$

The problem is thus reduced to the determination of the transition matrix elements between a bound state of the target atom and a scattering wave function with two outgoing electrons of definite asymptotic energy and angular momentum.

It is well-known that the difficult part of the problem is the accurate representation of the final continuum state. At low energies the Coulomb interaction of the two outgoing electrons must be fully taken into account up to very large radii. From

intermediate to high energies (typically 10 eV above the DPI threshold), however, the kinetic energy of the two electrons dominates over their repulsion already at few tens of atomic units from the ion. The two-body terms in the Hamiltonian can be, therefore, projected on an orthonormal L^2 two-particle basis set $\{\chi\}$ capable of representing all the relevant features of the two-particle states inside a spatial domain of radius R. This means to substitute the true repulsive potential with a projected potential:

$$V \rightarrow \tilde{V} \equiv |\chi\rangle \mathbf{V} \langle\chi| \qquad \mathbf{V} = \langle\chi| \frac{1}{r_{12}} |\chi\rangle \tag{6}$$

thus reducing the global Coulomb interaction to an effective three body potential in which the two electrons repel each other as long as both are within a radius R from the nucleus:

$$\tilde{V} \sim \frac{\theta(R - r_1)\,\theta(R - r_2)}{r_{12}} \tag{7}$$

Thanks to this drastic regularization of the potential, one can define a solvable Lippmann−Schwinger (LS) equation for the scattering wave function with outgoing-wave boundary conditions. For a two-electron atom the equation is

$$\psi^{-}_{\vec{k}_1\sigma_1\vec{k}_2\sigma_2,\Gamma} = \phi_{\vec{k}_1\sigma_1\vec{k}_2\sigma_2} + G_0^{-}(E)\tilde{V}\psi^{-}_{\vec{k}_1\sigma_1\vec{k}_2\sigma_2} \tag{8}$$

where $\phi_{\vec{k}_1\sigma_1\vec{k}_2\sigma_2}$ is an antisymmetrized ($\mathscr{A}$) product of two Coulomb waves:

$$\phi^{-}_{\vec{k}_1\sigma_1\vec{k}_2\sigma_2} = \sqrt{2}\mathscr{A}\,{}^2\phi^{-}_{\vec{k}_1\sigma_1}(\vec{r}_1,\zeta_1)\,{}^2\phi^{-}_{\vec{k}_2\sigma_2}(\vec{r}_2,\zeta_2) \tag{9}$$

defined as

$${}^2\phi^{-}_{\mathrm{k}\sigma}(\vec{r},\zeta) = \phi^{-}_{\mathrm{k}}(\vec{r})\,{}^2\chi_\sigma(\zeta) \tag{10}$$

$$\phi^{-}_{\mathrm{k}}(\vec{r}) = \frac{\mathrm{e}^{-\pi\gamma/2}\Gamma(1 - \mathrm{i}\gamma)}{(2\pi)^{3/2}} \mathrm{e}^{\mathrm{i}\vec{k}\cdot\vec{r}} F(\mathrm{i}\gamma|1|\mathrm{i}kr - \mathrm{i}\vec{k}\cdot\vec{r}) \tag{11}$$

with $\gamma = -Z/k$ and ${}^2\chi_\sigma(\zeta)$ a one-particle doublet spin function. The solutions of eq 8 can be expressed as linear combinations of independent irreducible tensorial components

$$\psi^{-}_{\vec{k}_1\sigma_1\vec{k}_2\sigma_2} = \sum_{\Gamma l_1 l_2} C^{S\Sigma}_{(1/2)\sigma_1(1/2)\sigma_2\zeta} \mathscr{Y}^{LM*}_{l_1 l_2}(\hat{k}_1,\hat{k}_2)\psi^{-\Gamma}_{l_1 k_1 l_2 k_2} \tag{12}$$

where $\mathscr{Y}^{LM}_{l_1 l_2}$ is a bipolar spherical harmonic:

$$\mathscr{Y}^{LM}_{l_1 l_2}(\hat{\Omega}_1,\hat{\Omega}_2) = \sum_{m_1 m_2} C^{LM}_{l_1 m_1 l_2 m_2} Y_{l_1 m_1}(\hat{\Omega}_1)\, Y_{l_2 m_2}(\hat{\Omega}_2) \tag{13}$$

and Γ specifies a complete set of good quantum numbers for spin and orbital angular momenta, their projections, and the parity: $\Gamma \equiv (S, L, \Sigma, M, \Pi)$. In real calculations, the sum in eq 12 is truncated by imposing the constraint $l_1, l_2 \le l_{\max}$, where $l_{\max}$ is the parameter which defines the expansion accuracy.

Within a specific symmetry, the LS equation becomes

$$\psi^{-\Gamma}_{k_1 l_1 k_2 l_2} = \phi^{-\Gamma}_{k_1 l_1 k_2 l_2} + G_0^{-}(E)\tilde{V}\psi^{-\Gamma}_{k_1 l_1 k_2 l_2} \tag{14}$$

where

$$\phi^{-\Gamma}_{k_1 l_1 k_2 l_2} = \frac{2}{\pi}[{}^2\phi^{-}_{k_1 l_1}(\vec{r}_1,\zeta_1) \wedge {}^2\phi^{-}_{k_2 l_2}(\vec{r}_2,\zeta_2)]^{S\Sigma}_{LM} \tag{15}$$

and the following normalization has been chosen

$$\begin{aligned}\langle\psi^{-\Gamma}_{l_1 k_1 l_2 k_2}|\psi^{-\Gamma}_{l_1' k_1' l_2' k_2'}\rangle = \langle\phi^{-\Gamma}_{l_1 k_1 l_2 k_2}|\phi^{-\Gamma}_{l_1' k_1' l_2' k_2'}\rangle = \frac{1}{k_1{}^2 k_2{}^2} \times \\ [\delta_{l_1 l_1'}\delta_{l_2 l_2'}\delta(k_1 - k_1')\,\delta(k_2 - k_2') - \\ \delta_{l_1 l_2'}\delta_{l_2 l_1'}\delta(k_1 - k_2')\,\delta(k_2 - k_1')]\end{aligned} \tag{16}$$

Since the interaction potential has been replaced by the projected potential $\tilde{V}$, the only quantity to be calculated is the projection of the LS wave function onto the chosen basis set:

$$\langle\chi|\psi^{-\Gamma}_{k_1 l_1 k_2 l_2}\rangle = \langle\chi|\phi^{-\Gamma}_{k_1 l_1 k_2 l_2}\rangle + \mathbf{G}^{-}_{0\Gamma}(E)\,\mathbf{V}\langle\chi|\psi^{-\Gamma}_{k_1 l_1 k_2 l_2}\rangle \tag{17}$$

with

$$\mathbf{G}^{-}_{0\Gamma}(E) = \langle\chi|G^{-}_{0\Gamma}(E)|\chi\rangle \tag{18}$$

The LS solution of eq 8 with outgoing-wave boundary conditions is given by

$$\psi^{-\Gamma}_{k_1 l_1 k_2 l_2} = \phi^{-\Gamma}_{k_1 l_1 k_2 l_2} + G^{-}_{0\Gamma}(E)|\chi\rangle\mathbf{V}[1 - \mathbf{G}^{-}_{0\Gamma}(E)\mathbf{V}]^{-1}\langle\chi|\phi^{-\Gamma}_{k_1 l_1 k_2 l_2}\rangle \tag{19}$$

Furthermore, by exploiting the fact that the target wave function in eq 1 is strongly localized even after applying the transition operator, one can use the following approximation:

$$\begin{aligned}\langle\phi_0||\mathscr{O}_1||\psi^{-\Gamma}_{k_1 l_1 k_2 l_2}\rangle \simeq \langle\phi_0||\mathscr{O}_1||\chi\rangle\langle\chi|\psi^{-\Gamma}_{k_1 l_1 k_2 l_2}\rangle = \\ \langle\phi_0||\mathscr{O}_1||\chi\rangle[1 - \mathbf{G}^{-}_{0\Gamma}(E)\mathbf{V}]^{-1}\langle\chi|\phi^{-\Gamma}_{k_1 l_1 k_2 l_2}\rangle\end{aligned} \tag{20}$$

This is the key equation of our method. It requires accurate calculations of the matrix elements of the two-particle Coulomb Green function, for which we have used the following identity resolution on a complete set of two-electron functions for the bound−bound, bound-continuum and continuum-continuum parts of the spectrum:

$$G^{\pm}_{0\Gamma}(E) = G^{bb}_{0\Gamma}(E) + G^{\pm,bc}_{0\Gamma}(E) + G^{\pm,cc}_{0\Gamma}(E) \tag{21}$$

where

$$G^{bb}_{0\Gamma}(E) = \sum_{nn'll'} \frac{|\Phi^{\Gamma}_{nn'll'}\rangle\langle\Phi^{\Gamma}_{nn'll'}|}{E - E_n - E_{n'}}$$

$$G^{\pm,bc}_{0\Gamma}(E) = \frac{2}{\pi}\sum_{nll'} \int_0^\infty k^2\,\mathrm{d}k\, \frac{|\Phi^{\Gamma\pm}_{nkll'}\rangle\langle\Phi^{\Gamma\pm}_{nkll'}|}{E - E_n - k^2/2 \pm \mathrm{i}0^+} \quad (22)$$

$$G^{\pm,cc}_{0\Gamma}(E) = \frac{4}{\pi^2}\sum_{ll'} \frac{1}{1+\delta_{ll'}} \int_0^\infty k^2\,\mathrm{d}k \int_0^\infty k'^2\,\mathrm{d}k' \frac{|\Phi^{\Gamma\pm}_{kk'll'}\rangle\langle\Phi^{\Gamma\pm}_{kk'll'}|}{E - k^2/2 - k'^2/2 \pm \mathrm{i}0^+} \quad (23)$$

The two-particle functions are defined as

$$|\Phi^{\Gamma}_{nn'll'}\rangle = [{}^2\phi_{nl} \wedge {}^2\phi_{n'l'}]^{\Gamma}[1(-)^{S+L}\delta_{ll'}\delta_{nn'}]^{-1/2} \quad (24)$$

$$|\Phi^{\Gamma\pm}_{nkll'}\rangle = [{}^2\phi_{nl} \wedge {}^2\phi^{\pm}_{kl'}]^{\Gamma} \quad (25)$$

$$|\Phi^{\Gamma\pm}_{kkll'}\rangle = [{}^2\phi^{\pm}_{kl} \wedge {}^2\phi^{\pm}_{k'l'}]^{\Gamma} \quad (26)$$

with

$$[{}^2\phi_{xl} \wedge {}^2\phi_{xT}]^{\Gamma} \equiv \sqrt{2}\mathcal{A}\sum_{mm'}\sum_{\sigma\sigma'} C^{LM}_{lm,l'm'} C^{S\Sigma}_{(1/2)\sigma,(1/2)\sigma'} \times {}^2\phi_{xlm\sigma}\,{}^2\phi_{x'l'm'\sigma'} \quad (27)$$

where ${}^2\phi_{nlm\sigma}$ and ${}^2\phi^{\pm}_{klm\sigma}$ are hydrogen-like bound and continuum functions in the field of a nuclear charge Z (see Appendix A).

To evaluate the right-hand side of eq 20, it is necessary to represent accurately the exact unperturbed two-particle Coulomb Green function using an appropriate projection basis set $\{\chi\}$. In the present calculations, the Green function has been expressed in terms of 500 bound and 1000 continuum states, whose linear momenta are suitably chosen (for each basis function) in the interval $[10^{-4}, 10^3]$ au so to faithfully reproduce the Coulomb transform of the wave function itself. This means that the final wave function is expanded over roughly two million states for each orbital angular momentum. The overlap between basis functions and Coulomb functions is obtained by interpolation. The integrals in eqs 22 and 23 are then evaluated numerically using standard quadratures.

Finally, we observe that the unperturbed part of the LS wave function 19, expressed as the product of two continuum Coulomb functions, is orthogonal to any single-ionization close-coupling function, since both refer to the same residual charge of the parent ion. The fact that this choice of the charge might be effective to eliminate spurious contributions from the single-ionization channels and to reduce the dimension of the interaction box has been already pointed out in refs 22 and 46.

III. Generalization to Many-Electron Atoms

The generalization of the method to many-electron atoms is straightforward in the case of DPI processes in which the state of the grandparent ion is total-symmetric and energetically well isolated, as for example in the case of photoionization of the valence shell of alkaline-earths atoms. The main difference with the helium case is that the unperturbed continuum functions are no longer ordinary Coulomb functions, but they have to be orthogonal to the wave function of the parent ion itself.

For nontotally symmetric cases, or when the grandparent ion itself can exist in different excited states, as for example in the case of rare gases with a double hole in the valence shell, it is still possible to define orthogonal two-electron channels, each one associated to a different grand-parent ion state. The formal generalization of eq 8 is given by

$$\psi^{-}_{\alpha,k_1l_1k_2l_2} = \phi^{-}_{\alpha,k_1l_1k_2l_2} + \sum_{\gamma} G^{-}_{0\gamma}(E) V_{\gamma\alpha} \psi^{-}_{\alpha,k_1l_1k_2l_2} \quad (28)$$

and eq 20 becomes

$$\langle\phi_0||\mathcal{O}_1||\psi^{-}_{\alpha,k_1l_1k_2l_2}\rangle \simeq \langle\phi_0||\mathcal{O}_1||\chi\rangle[1 - \sum_{\gamma}\mathbf{G}^{-}_{0\gamma}(E)\mathbf{V}_{\gamma\alpha}]^{-1}\langle\chi|\phi^{-}_{\alpha,k_1l_1k_2l_2}\rangle \quad (29)$$

IV. Results and Discussion

In this section, we compare TDCS of helium DPI calculated using our method with the corresponding angular distributions measured by Knapp et al.[47] at an excess energy of 100 eV in equal and unequal energy sharing. In these measurements, the uncertainty on the emission direction of the first (reference) electron is ±5° around the nominal values (±3° for $\theta_1 = 45°$) and the uncertainty on its energy is ±5 eV; the angular distributions of the complementary electron are within the plane defined by the polarization vector and the reference electron within ±15° (±5° for $\theta_1 = 0°$). Our TDCS are given in barn/(eV rad), the standard units for the 4-fold differential cross sections, their comparison with those of ref 47, normalized to the total cross section measured in refs 48 and 49, requires the multiplication of the measured TDCS by a factor 10. This difference should probably reduce appreciably by convoluting the theoretical TDCS with the experimental uncertainties. We point out, indeed, that the order of magnitude of our TDCS is in close agreement with that of the TDCS measured by Turri et al.[50] at excess energy of 80 eV with higher energy and angular resolution, and normalized to accurate CCC calculations.

The matrix elements of the two-particle Coulomb Green function and of the projected potential have been calculated using a basis set of B-spline of order $k = 8$, defined on knots of uniform asymptotic spacing (0.75 au) and short-range spacing chosen to optimize the helium ground state. (See ref 51 for a detailed definition of the parameters characteristic of a B-splines basis set.)

In order to examine the convergence of the method with respect to the two main parameters: box radius (R) and largest orbital angular momentum (l_{max}), we have carried out calculations with 28.8 au $\leq R \leq$ 40 au and $4 \leq l_{max} \leq 6$, in both acceleration and velocity gauge. In Figure 1, we compare the calculated TDCS with the angular distribution measured in unequal energy sharing ($E_1 = 30$ eV, $E_2 = 70$ eV) and reference electron collected along the polarization direction of the incident light ($\theta_1 = 0°$, somewhat the most demanding angular configuration in terms of interelectronic correlation). A few trends emerge from the inspection of Figure 1:

- As the box radius increases, the two major lobes squeeze and approach the experimental ones.
- The spurious lobe in the forward direction (kinematically favored but depressed by the electron repulsion) disappears as larger orbital angular momenta (i.e., more electron correlation) are included in the calculation.

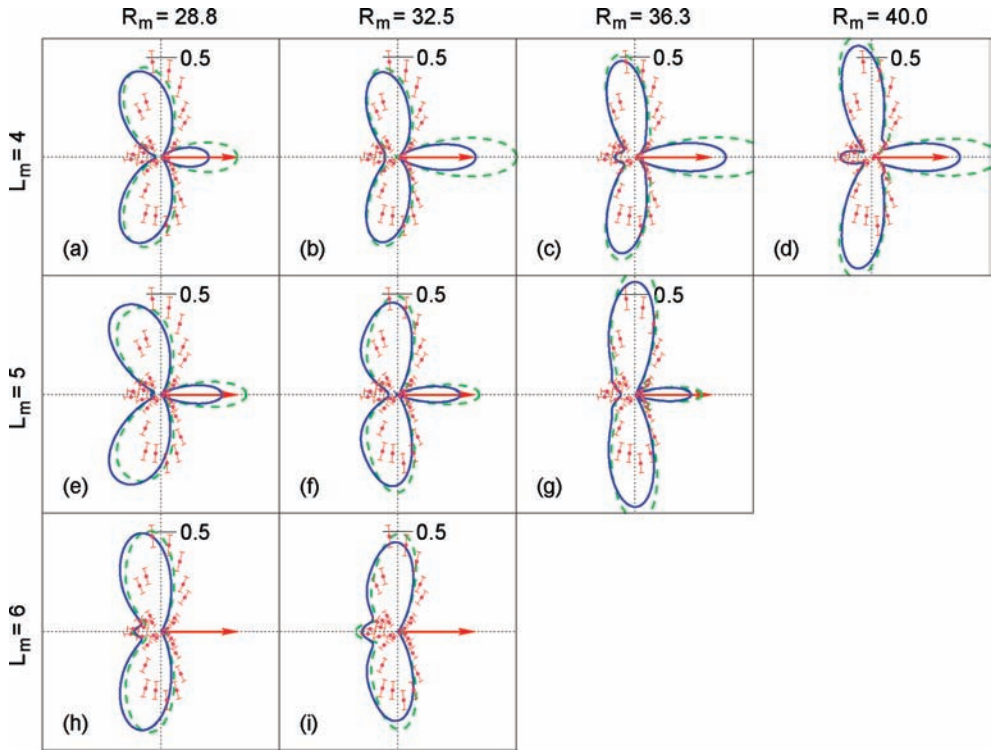

Figure 1. Four-fold differential cross section of the helium DPI on absolute scale in [barn/(eV rad)] measured in unequal energy sharing ($E_1 = 30$ eV, $E_2 = 70$ eV), and calculated with our method for different values of the box radius (R_m) and maximum angular momentum (L_m). The arrows indicate the direction of emission ($\theta_1 = 0°$) of the reference electron with respect to the polarization direction of the incident light. The points with error bars are experimental values[47] multiplied by a factor 10, the continuous line is the TDCS calculated in acceleration gauge, the dashed line in velocity gauge.

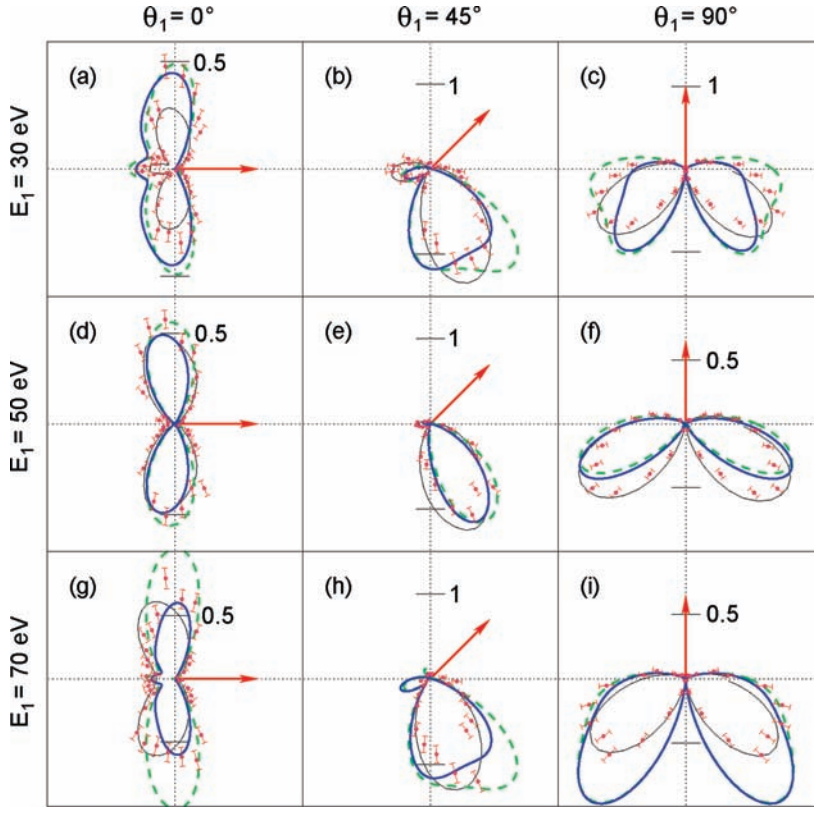

Figure 2. Four-fold differential cross section of the helium DPI on absolute scale in [barn/(eV rad)] measured in equal and unequal energy sharing and calculated with box radius $R = 32.5$ and maximum angular momentum $l_{max} = 6$. The arrow indicates the direction of emission of the reference electron with respect to the polarization direction of the incident light. The points with error bars are the experimental values[47] multiplied by a factor 10, the continuous line is the TDCS calculated in acceleration gauge, the dashed line in velocity gauge. The thin continuous line is the TDCS calculated in ref 47 with the CCC method.

- With the set of parameters ($R_m = 32.5$ au, $l_{max} = 6$) that better reproduce the measured angular distribution in these test calculations, the agreement between the two gauges is quite good both in shape and in absolute value. Notice that the TDCS calculated in the length gauge (not reported here) have lobes generally larger and less regular than in the other two gauges. Similar evidence have been reported also by Kheifets and Bray.[32]

In Figure 2, we compare our TDCS, calculated with $R_m = 32.5$ au and $l_{max} = 6$, with angular distributions measured[47] at equal energy sharing ($E_1 = E_2 = 50$ eV) and two (complementary) unequal energy sharings: ($E_1 = 30$ eV, $E_2 = 70$ eV), ($E_1 = 70$ eV, $E_2 = 30$ eV) for three emission directions of the first electron ($\theta_1 = 0°, 30°, 60°$). For comparison, in the same figure, we plot also the TDCS calculated in ref 47 with the CCC method.

We see that, in the case of equal energy sharing, the agreement between our TDCS and the measured ones is pretty good for each emission direction of the primary electron. In unequal energy sharing, the agreement is noteworthy for $\theta_1 = 0°$, mainly in the acceleration gauge, while for larger angles it becomes less satisfactory. The comparison between our results and the CCC calculations of ref 47 indicates a better quality of the latter only at $\theta_1 = 90°$. These facts suggest the need of including higher angular momenta and probably also of extending the box radius to improve the quality of the results obtained with our method.

V. Conclusions

A new method based on the solution of a Lippmann−Schwinger equation with two-particle Coulomb Green function and projected interelectronic potential has been proposed to calculate DPI TDCS of atoms. Preliminary results obtained for helium DPI have been compared with measured and calculated angular distributions at equal and unequal energy sharing.

The analysis of these results indicates that a proper choice of the two main parameters of the method: box radius and largest angular momentum, allows one to obtain sufficiently accurate results with a modest computational effort. Considering that other parameters are available, such as those characteristic of the L^2 basis set used for the matrix representations, and plenty of room is available to improve the present implementation of the method, we are confident that the level of accuracy can be largely increased without increasing too much the required computational effort.

We point out that this method is also appealing because it provides a clear computational scheme that can be applied also to the calculation of DPI TDCS of many-electron atoms.

Acknowledgment. We gratefully acknowledge the financial support of the Italian MURST PRIN 2006.

Appendix A: Hydrogen-Like Bound and Continuum Functions

The hydrogen-like bound and continuum functions in the field of a nuclear charge Z are defined in terms of the confluent hypergeometric function: $F_{nl}(2Zr/n)$, and the regular continuum Coulomb radial function: $F_l(\gamma;\rho)$, respectively, as follows

$$\phi_{nlm}(\vec{r}) = Z^{3/2} N_{nl} F_{nl}\left(\frac{2Zr}{n}\right) Y_{lm}(\hat{r}) \tag{A1}$$

$$N_{nl} = \frac{2}{n^2}\sqrt{\frac{(n-l-1)!}{(n+l)!}} \tag{A2}$$

$$F_{nl}(x) = x^l e^{-x/2} L_{n-l-1}^{2l+1}(x) \tag{A3}$$

$$L_p^k(z) = \binom{p+k}{k} F(-p|k+1|z) \tag{A4}$$

$$F(\alpha|\beta|\gamma) = \sum_{n=0}^{\infty} \frac{\Gamma(\alpha+n)\,\Gamma(\beta)}{\Gamma(\alpha)\,\Gamma(\beta+n)} \frac{z^n}{n!} \tag{A5}$$

and

$${}^2\phi_{klm\sigma}^-(\vec{r},\zeta) = \phi_{klm}^-(\vec{r})\chi_\sigma(\zeta) \tag{A6}$$

$$\phi_{klm}^-(\vec{r}) = i^l e^{-i\sigma_l}\phi_{klm}(\vec{r}) \tag{A7}$$

$$\phi_{klm}(\vec{r}) = \frac{F_l(\gamma;kr)}{kr} Y_{lm}(\hat{r}) \tag{A8}$$

$$F_l(\gamma;\rho) = 2^l e^{-\pi\gamma/2} \frac{|\Gamma(l+1+i\gamma)|}{(2l+1)!} e^{i\rho}\rho^{l+1} \times F(l+1+i\gamma|2l+2|-2i\rho) \tag{A9}$$

The adopted normalization conditions are the following

$$\langle {}^2\phi_{nlm\sigma}|^2\phi_{n'l'm'\sigma'}\rangle = \delta_{nn'}\delta_{ll'}\delta_{mm'}\delta_{\sigma\sigma'} \tag{A10}$$

$$\langle {}^2\phi_{klm\sigma}|^2\phi_{k'l'm'\sigma'}\rangle = \frac{\pi}{2k^2}\delta(k-k')\delta_{ll'}\delta_{mm'}\delta_{\sigma\sigma'} \tag{A11}$$

References and Notes

(1) Schwarzkopf, O.; Krässig, B.; Elmiger, J.; Schmidt, V. *Phys. Rev. Lett.* **1993**, *70*, 3008.
(2) Avaldi, L.; Huetz, A. *J. Phys. B* **2005**, *38*, S861.
(3) Krässig, B.; Schaphorst, S. J.; Schwarzkopf, O.; Scherer, N.; Schmidt, V. *J. Phys. B* **1996**, *29*, 4255.
(4) Schaphorst, S. J.; Jean, A.; Schwarzkopf, O.; Lablanquie, P.; Andric, L.; Huetz, A.; Mazeau, J.; Schmidt, V. *J. Phys. B* **1996**, *29*, 1901.
(5) Rudge, M. R. H.; Seaton, M. J. *Proc. R. Soc. A* **1965**, *283*, 262.
(6) Brauner, M.; Briggs, J. S.; Klar, H. *J. Phys. B* **1989**, *22*, 2265.
(7) Maulbetsch, F.; Briggs, J. S. *Phys. Rev. Lett.* **1992**, *68*, 2004.
(8) Maulbetsch, F.; Briggs, J. S. *J. Phys. B* **1993**, *26*, L647.
(9) Maulbetsch, F.; Briggs, J. S. *J. Phys. B* **1993**, *26*, 1679.
(10) Berakdar, J.; Briggs, J. S. *Phys. Rev. Lett.* **1994**, *72*, 3799.
(11) Lucey, S. P.; Rasch, J.; Whelan, C. T.; Walters, H. R. J. *J. Phys. B* **1998**, *31*, 1237.
(12) Lucey, S. P.; Rasch, J.; Whelan, C. T. *Proc. R. Soc. A* **1965**, *455*, 349.
(13) Proulx, D.; Shakeshaft, R. *Phys. Rev. A* **1993**, *48*, 875(R).
(14) Pont, M.; Shakeshaft, R. *Phys. Rev. A* **1995**, *51*, 2676(R).
(15) Pont, M.; Shakeshaft, R.; Maulbetsch, F.; Briggs, J. S. *Phys. Rev. A* **1996**, *53*, 3671.
(16) Horner, D. A.; Colgan, J.; Martín, F.; McCurdy, C. W.; Pindzola, M. S.; Rescigno, T. N. *Phys. Rev. A* **2004**, *70*, 06401.
(17) Malegat, L.; Selles, P.; Kazansky, A. *Phys. Rev. A* **1999**, *60*, 3667.
(18) Malegat, L.; Selles, P.; Kazansky, A. K. *Phys. Rev. Lett.* **2000**, *85*, 4450.
(19) Selles, P.; Malegat, L.; Kazansky, A. K. *Phys. Rev. A* **2002**, *65*, 032711.
(20) Collins, S. A.; et al. *Phys. Rev. A* **2002**, *65*, 052717.
(21) Baertschy, M.; Rescigno, T. N.; McCurdy, C. W. *Phys. Rev. A* **2001**, *64*, 022709.
(22) McCurdy, C. W.; Rescigno, T. N. *Phys. Rev. A* **2000**, *62*, 032712.

(23) Citrini, F.; Malegat, L.; Selles, P.; Kazansky, A. K. *Phys. Rev. A* **2003**, *67*, 042709.
(24) Pindzola, M. S.; Schultz, D. R. *Phys. Rev. A* **1996**, *53*, 1525.
(25) Pindzola, M. S.; Robicheaux, F. *Phys. Rev. A* **1998**, *57*, 318.
(26) Colgan, J.; Pindzola, M. S.; Robicheaux, F. *J. Phys. B* **2001**, *34*, L457.
(27) Colgan, J.; Pindzola, M. S. *Phys. Rev. A* **2002**, *65*, 032729.
(28) Colgan, J.; Foster, M.; Pindzola, M. S.; Robicheaux, F. *J. Phys. B* **2007**, *40*, 4391.
(29) Colgan, J.; Pindzola, M. S. *Phys. Rev. A* **2002**, *65*, 022709.
(30) Bray, I.; Stelbovics, A. T. *Phys. Rev. Lett.* **1992**, *69*, 53.
(31) Bray, I.; Stelbovics, A. T. *Phys. Rev. Lett.* **1993**, *70*, 746.
(32) Kheifets, A. S.; Bray, I. *Phys. Rev. A* **1996**, *54*, 995(R).
(33) Konovalov, D. A.; Bray, I.; McCarthy, I. E. *J. Phys. B* **1994**, *27*, L413.
(34) Bräuning, H.; 1998, *31*, 5149.
(35) Cvejanoviç, S.; Wightman, J. P.; Reddish, T. J.; Maulbetsch, F.; MacDonald, M. A.; Kheifets, A. S.; Bray, I. *J. Phys. B* **2000**, *33*, 265.
(36) Rescigno, T. N.; McCurdy, C. W.; Isaacs, W. A.; Baertschy, M. *Phys. Rev. A* **1999**, *60*, 3740.
(37) Bray, I. *Phys. Rev. Lett.* **1997**, *78*, 4721.
(38) Bray, I. *Phys. Rev. Lett.* **2002**, *89*, 273201.
(39) McCurdy, C. W.; Rescigno, T. N.; Byrum, D. *Phys. Rev. A* **1997**, *56*, 1958.
(40) McCurdy, C. W.; Horner, D. A.; Rescigno, T. N.; Martín, F. *Phys. Rev. A* **2004**, *69*, 032707.
(41) McCurdy, C. W.; Baertschy, M.; Rescigno, T. N. *J. Phys. B* **2004**, *37*, R137.
(42) Colle, R.; Simonucci, S. *J. Phys. B* **2002**, *35*, 4033.
(43) Huetz, A.; Selles, P.; Waymel, D.; Mazeau, J. *J. Phys. B* **1991**, *24*, 1917.
(44) L Malegat, P. S.; Huetz, A. *J. Phys. B* **1997**, *30*, 251.
(45) Malegat, L.; Selles, P.; Lablanquie, P.; Mazeau, J.; Huetz, A. *J. Phys. B* **1997**, *30*, 263.
(46) McCurdy, C. W.; Horner, D. A.; Rescigno, T. N. *Phys. Rev. A* **2001**, *63*, 022711.
(47) Knapp, A.; et al. *J. Phys. B* **2005**, *38*, 615.
(48) Samson, J. A. R.; He, Z. X.; Yin, L.; Haddad, G. N. *J. Phys. B* **1994**, *27*, 887.
(49) Samson, J. A. R.; Stolte, W. C.; He, Z. X.; Cutler, J. N.; Lu, Y.; Bartelatt, R. J. *Phys. Rev. A* **1998**, *57*, 1906.
(50) Turri, G.; Avaldi, L.; Bolognesi, P.; Camilloni, R.; Coreno, M.; Berakdar, J.; Kheifets, A. S.; Stefani, G. *Phys. Rev. A* **2002**, *65*, 034702.
(51) Argenti, L.; Colle, R. *Comput. Phys. Commun.* **2009**, 1, DOI: 10.1016/j.cpc.2009.03.002.

JP905155W